ilmedia

TECHNISCHE UNIVERSITÄT
ILMENAU

Meier, Lukas; Braun, Christian; Hannappel, Thomas; Schmidt, W. Gero

Band alignment at GaxIn1-xP/AlyIn1-yP alloy interfaces from hybrid density functional theory calculations

Original published in:	Physica status solidi. B, Basic research. - Weinheim : Wiley-VCH. - 258 (2021), 2, art. 2000463, 4 pp.
Original published:	2020-10-06
ISSN:	1521-3951
DOI:	10.1002/pssb.202000463
[*Visited:*	2021-11-26]

This work is licensed under a Creative Commons Attribution 4.0 International license. To view a copy of this license, visit https://creativecommons.org/licenses/by/4.0/

TU Ilmenau | Universitätsbibliothek | ilmedia, 2022
http://www.tu-ilmenau.de/ilmedia

physica status solidi b
www.pss-b.com

Band Alignment at $Ga_xIn_{1-x}P/Al_yIn_{1-y}P$ Alloy Interfaces from Hybrid Density Functional Theory Calculations

Lukas Meier, Christian Braun, Thomas Hannappel, and Wolf Gero Schmidt**

The composition dependence of the natural band alignment at the $Ga_xIn_{1-x}P/Al_yIn_{1-y}P$ alloy interface is investigated via hybrid functional based density functional theory. The direct–indirect crossover for the $Ga_xIn_{1-x}P$ and $Al_yIn_{1-y}P$ alloys is calculated to occur for $x = 0.9$ and $y = 0.43$. The calculated $Ga_xIn_{1-x}P/Al_yIn_{1-y}P$ interface band alignment shows a crossover from type-I to type-II with increasing Ga content x. The valence band offset is essentially positive irrespective of the alloy compositions, and amounts up to 0.56 eV. The conduction band offset varies between −0.85 and 1.16 eV.

1. Introduction

The III–V compound semiconductors play an important role for a variety of electronic and optoelectronic devices such as high electron mobility and heterostructure bipolar transistors, diode lasers, light-emitting diodes, photodetectors, electro-optic modulators, and frequency-mixing components. Apart from the binary compounds, ternary and quaternary alloys also may be combined within a countless variety of heterostructure configurations. The efficient exploitation of this flexibility requires, however, knowledge not only of the electronic properties of single compounds and alloys[1] and their surfaces[2] but also information on the band alignment of the respective interfaces.[3–7]

This motivates this article, which addresses the stoichiometry-dependent band alignment at the $Ga_xIn_{1-x}P/Al_yIn_{1-y}P$ alloy interface. This interface occurs, e.g., in heterostructure solar cells and tandem absorber structures for the direct solar-to-hydrogen conversion.[8] GaP and AlP have indirect bandgaps of 2.34–2.35[9,10] and 2.5 eV,[11] respectively, at zero temperature. In contrast, InP is a direct-gap semiconductor with a low-temperature bandgap of 1.42 eV.[12] According to photoluminescence data,[13] the Ga content of $Ga_xIn_{1-x}P$ at the direct–indirect bandgap crossover is at about $x = 0.71$. Measurements for $Al_yIn_{1-y}P$ indicate the direct–indirect crossover for $y = 0.41$,[14] whereas recent density functional calculations place it at $y = 0.48$.[15]

To the best of our knowledge, there are neither experimental nor theoretical data available on the relative positions of the valence band maxima (VBM) and conduction band minima (CBM) at the $Ga_xIn_{1-x}P/Al_yIn_{1-y}P$ alloy interface, apart from valence band offsets at the binary end points.[3,4] This article aims at closing this gap by providing band alignment values for the complete composition range. We focus here on the "natural" band lineups between unstrained materials obtained from the branch-point energies of the respective materials.[16–21] They are determined here within hybrid density functional theory (DFT).

2. Methodology

In detail, DFT calculations are performed using the Vienna ab initio simulation package (VASP).[22] The generalized gradient approximation (GGA) as well as hybrid functionals is used to model the electron exchange and correlation interaction. In particular, the revised Perdew–Becke–Ernzerhoff (PBEsol)[23] GGA functional and the Heyd–Scuseria–Ernzerhof (HSE) hybdrid functional[24] are used for structural relaxations and electronic structure calculations, respectively. In the latter, the fraction of exact exchange is increased to 29% for a better match with the measured bandgaps. **Table 1** shows a comparison of the direct and indirect bandgaps of AlP, GaP, and InP calculated here with experimental data. It can be seen that the fundamental bandgap for all three semiconductors is well described with hybrid DFT, within about 0.1 eV, whereas larger deviations occur for higher transitions. The electron–ion interaction is described by the projector-augmented wave (PAW) scheme.[25,26] The electronic wave functions are expanded into plane waves up to a kinetic energy cutoff of 650 eV. The Brillouin-zone integration is performed using the Monkhorst–Pack scheme with a k-point density of $2 \times 2 \times 2$. The ternary alloys are modeled by rhombohedral 16 atom unit cells. To take the different realizations of a given stoichiometry of the group-III ions into account, the calculated band-edge energies are averaged accounting for their respective statistical weights.

L. Meier, C. Braun, Prof. W. G. Schmidt
Lehrstuhl für Theoretische Materialphysik
Universität Paderborn
33095 Paderborn, Germany
E-mail: lukasme5@mail.upb.de; W.G.Schmidt@upb.de

Prof. T. Hannappel
Institut für Physik
Technische Universität Ilmenau
Gustav-Kirchhoff-Straße 5, 98693 Ilmenau, Germany

The ORCID identification number(s) for the author(s) of this article can be found under https://doi.org/10.1002/pssb.202000463.

© 2020 The Authors. Physica Status Solidi B published by Wiley-VCH GmbH. This is an open access article under the terms of the Creative Commons Attribution License, which permits use, distribution and reproduction in any medium, provided the original work is properly cited.

The copyright line for this article was changed on 18 December 2020 after original online publication.

DOI: 10.1002/pssb.202000463

Table 1. Comparison of the minimum electronic transition energies (in eV) between valence and conduction states of AlP, GaP, and InP calculated here on the GGA and hybrid level of theory with experimental data as cited in ref. [28].

	AlP		GaP		InP	
	$\Gamma-\Gamma$	$\Gamma-X$	$\Gamma-\Gamma$	$\Gamma-X$	$\Gamma-\Gamma$	$\Gamma-X$
GGA	2.37	1.45	1.59	1.55	0.48	1.37
Hybrid	3.44	2.49	2.62	2.49	1.41	2.30
Exp.	3.63	2.51	2.90	2.35	1.42	2.44

The AlP, GaP, and InP calculations are performed at the respective equilibrium lattice parameters of 5.473, 5.476, and 5.932 Å, which are close to the corresponding low-temperature experimental values of 5.464, 5.451, and 5.869 Å. The lattice constants of the ternary alloys have been interpolated linearly between the binary compounds according to Vegard's law. To estimate the band discontinuities, the valence and conduction band edges are aligned to the branch-point energies of the respective systems. Following Schleife et al.,[5] the branch-point energy is approximated here as

$$E_{\mathrm{bp}} \approx \frac{1}{2N_K}\sum_k\left[\frac{1}{N_{\mathrm{vb}}}\sum_i^{N_{\mathrm{vb}}}\varepsilon_{v_i}(k)+\frac{1}{N_{\mathrm{cb}}}\sum_j^{N_{\mathrm{cb}}}\varepsilon_{c_j}(k)\right] \tag{1}$$

where N_k is the number of **k** points used to sample the Brillouin zone and ε_{v_i} and ε_{c_j} are the ith highest valence and jth lowest conduction band states at the wave vector **k**, respectively. Here, the 16 highest valence and the 8 lowest conduction states are included in the calculation of the branch-point energies for the 16 atom unit cells.

3. Results and Discussion

The band structures of $Ga_xIn_{1-x}P$ calculated on the DFT–GGA level of theory for the binary end points as well as $x = 0.875$ are shown in **Figure 1**. To ease the interpretation, the bands of the 16 atom unit cell are unfolded in the Brillouin zone of the primitive unit cell.[27] It is found that the indirect–direct crossover in the band structure occurs for Ga-rich alloys, in agreement with experimental data.[13]

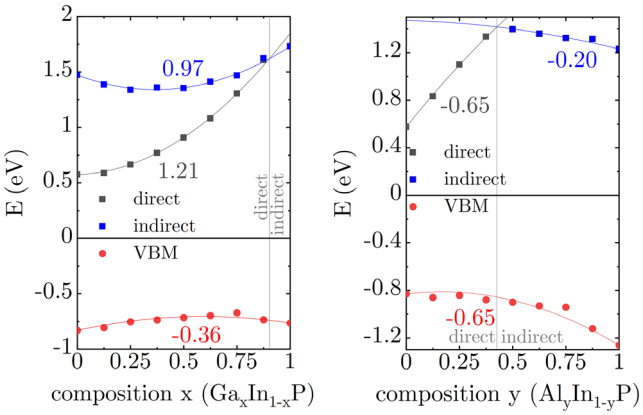

Figure 2. Composition dependence of branch-point aligned valence and conduction band energies of $Ga_xIn_{1-x}P$ (lhs) and $Al_yIn_{1-y}P$ (rhs) calculated within hybrid DFT. The solid lines result from fits to Equation (2). The bowing parameters (in eV) as well as the direct–indirect crossover compositions are indicated.

To determine the critical x_c more precisely, we perform hybrid DFT calculations. The calculated band-edge energies giving rise to direct and indirect transitions are shown in **Figure 2** (lhs), and have been fitted using the expression

$$E(x) = E_1x + E_0(1-x) - bx(1-x) \tag{2}$$

where E_1 and E_0 are the energies of the binary end points. We calculate a considerable positive bowing of the order of 1 eV for the conduction band energies: values of $b_\Gamma = 1.21$ eV for the conduction band energies at the Γ point and $b_X = 0.97$ eV at the X point are determined here. The bowing is less pronounced for the valence band, $b_\Gamma = -0.36$ eV. The direct–indirect crossover is calculated to occur for rather Ga-rich samples, i.e., for $x_c = 0.9$. We are not aware of previous theoretical findings in that respect. A value of $x_c = 0.71$ has been concluded from photoluminescence data.[13] Theoretical data are available, however, for the GaP/InP valence band offset: based on the alignment with respect to the core levels, Wei and Zunger[3] and Li et al.[4] calculated 0.11 and 0.47 eV, respectively. The present value of −0.07 eV supports the early prediction by Zunger.

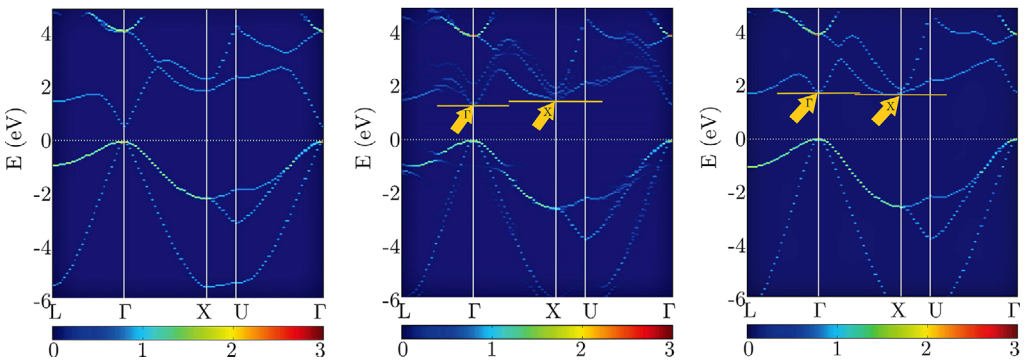

Figure 1. Band structures of GaP, $Ga_{0.875}In_{0.125}P$, and InP (from left to right) calculated on the DFT–GGA level of theory. The bands are unfolded into the 1×1 Brillouin zone following the study by Medeiros et al.[27] Arrows indicate the crossover.

© 2020 The Authors. Physica Status Solidi B published by Wiley-VCH GmbH

A similar analysis has been performed for $Al_yIn_{1-y}P$, see data shown in Figure 2 (rhs). Here, smaller and negative parameters have been determined for the conduction band bowing, $b_\Gamma = -0.65$ eV and $b_X = -0.2$ eV, whereas the valence band bowing is more pronounced than for $Ga_xIn_{1-x}P$. The present calculations result in $b_\Gamma = -0.65$ eV. The direct–indirect crossover is calculated to occur for intermediate stoichiometries, i.e., for $y_c = 0.43$. This is in between the value determined by photoluminescence spectroscopy, $y_c = 0.41$[14] and previous calculations that obtained $y_c = 0.48$.[15] Again, the valence band offset for the binary end points can be compared with previous theory based on the alignment with respect to the core levels. The AlP/InP interface valence band offsets were predicted to amount to 0.65 and 1.00 eV, respectively, in the studies by Wei and Zunger and Li et al.[3,4]. Our value of 0.43 supports the early finding by Zunger.

Obviously, the stoichiometry dependence of the $Ga_xIn_{1-x}P$ and $Al_yIn_{1-y}P$ band edges is different. The conduction band energy of $Al_yIn_{1-y}P$ increases for $0 \leq y \leq 0.43$ until a maximum value of 1.42 eV is reached at $y_c = 0.43$. For higher Al content, the conduction band energy decreases rather linearly. In contrast, the fundamental conduction band energy of $Ga_xIn_{1-x}P$ increases monotonically and with considerable bowing over the entire composition range. The valence band energies, on the other hand, are relatively independent of the stoichiometry for $Ga_xIn_{1-x}P$ and decrease almost monotonically with strong bowing over the entire composition range for $Al_yIn_{1-y}P$.

The calculated valence and conduction band energies of $Ga_xIn_{1-x}P$ and $Al_yIn_{1-y}P$ can now be used to predict the composition-dependent band alignment at $Ga_xIn_{1-x}P/Al_yIn_{1-y}P$ alloy interfaces. Figure 1 shows the calculated natural valence and conduction band offsets at the interface over the entire composition range. Thereby, we follow the notation that positive band offsets correspond to the situation that the band-edge energy of $Ga_xIn_{1-x}P$ is above the respective band-edge energy of $Al_yIn_{1-y}P$.

The valence band offsets are positive for almost the complete composition range, apart from a very narrow range characterized by a minute concentration of Ga in $Ga_xIn_{1-x}P$ and about 20% Al in $Al_yIn_{1-y}P$, see gray area in the upper plot of **Figure 3**. Furthermore, the valence band offsets increase with growing Al concentration and are highest for medium Ga concentrations around 50%. The maximum valence band offset of 0.56 eV is reached for the $AlP/Ga_{0.6}In_{0.4}P$ interface.

In contrast to the (almost) purely positive valence band offsets, the conduction band offsets may be positive and negative for a broad range of stoichiometric combinations, see lower plot in Figure 3. The maximum value of 1.16 eV is realized for GaP/InP interfaces, whereas the minimum of −0.85 eV is predicted for $InP/Al_{0.43}In_{0.57}P$ heterostructures.

Both type-I and type-II heterojunctions can be realized with $Ga_xIn_{1-x}P/Al_yIn_{1-y}P$ interfaces, as shown in Figure 3. A further classification is obtained by considering the character of the fundamental bandgap in the respective alloys. The combinations direct–direct, direct–indirect, indirect–direct, and indirect–indirect can be realized for suitable chosen stoichiometries as shown in Figure 3. The stoichiometries leading to direct–direct combinations ($x \leq 0.90 \wedge y \leq 0.43$) as well as indirect–direct combinations ($x \leq 0.90 \wedge y \geq 0.43$) can lead to negative as well as positive conduction band offsets.

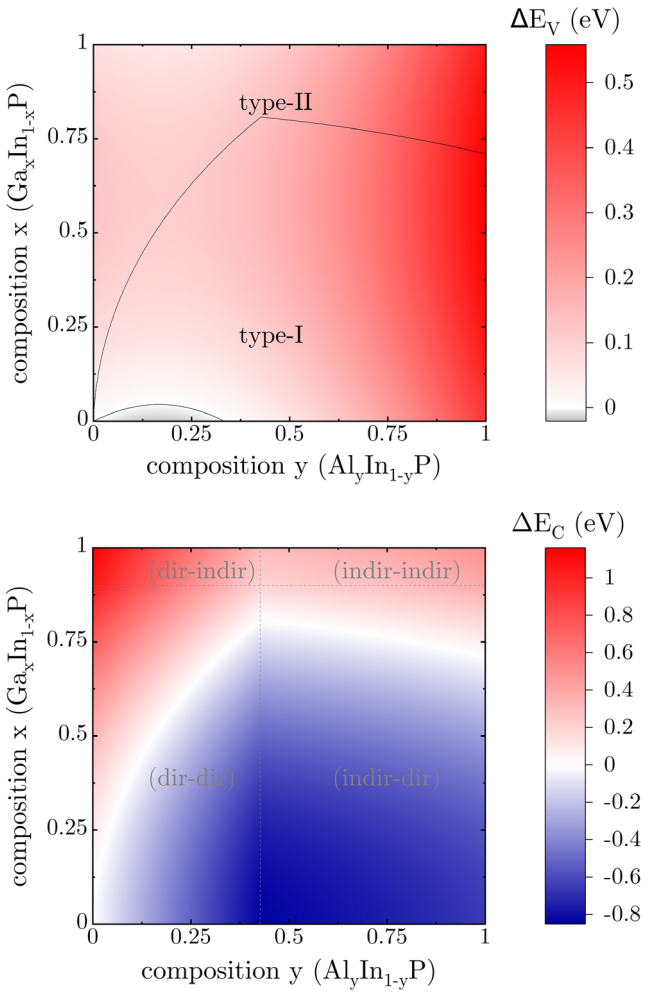

Figure 3. Valence (top) and and conduction band offsets (bottom) for the $Al_xIn_{1-x}P/Ga_yIn_{1-y}P$ alloy interface in dependence on the stoichiometry calculated on the hybrid level of theory.

Effects of strain or dipoles as well as atomic reordering may modify the band lineup at real interfaces. To roughly estimate the influence strain may have on the band alignment, we perform calculations for uniformly strained AlP and InP compounds, assuming a common lattice constant of 5.703 Å at the interface. This changes the valence and conduction band offsets from 0.43 to 0.47 eV and from −0.66 to −0.04 eV, respectively. Obviously, the conduction band offsets are very susceptible to strain engineering, whereas the valence band offsets seem more robust.

4. Conclusion

In summary, the band structures of $Ga_xIn_{1-x}P$ and $Al_yIn_{1-y}P$ alloys and the band alignment at the respective interfaces have been calculated within hybrid DFT. The calculated direct–indirect crossover points of $x = 0.9$ and $y = 0.43$ for the ternary compounds are consistent with the experimental data and

© 2020 The Authors. Physica Status Solidi B published by Wiley-VCH GmbH

previous theoretical work. The band offsets at the alloy interface can be tuned over a wide energy range. Although the conduction band offsets are positive for nearly the complete composition range, the valence band offset varies between −0.85 eV and 1.16 eV. This allows for the realization of both type-I and type-II heterostructures. An additional degree of freedom for the interface engineering is provided by the possibility to combine materials with direct and indirect fundamental gaps. Interface strain can be expected to affect, in particular, the conduction band offsets.

Acknowledgements

Financial support by DFG (PAK981, SCHM1361/26) is gratefully acknowledged. The authors thank the Paderborn Center for Parallel Computing (PC^2) and the Höchstleistungs-Rechenzentrum Stuttgart (HLRS) for grants of high-performance computer time. Open access funding enabled and organized by Projekt DEAL.

Conflict of Interest

The authors declare no conflict of interest.

Keywords

AlInP, band alignment, computational physics, density functional theory, GaInP, heterostructures, interfaces

Received: August 25, 2020
Revised: September 21, 2020
Published online: October 29, 2020

[1] I. Vurgaftman, J. R. Meyer, L. R. Ram-Mohan, *J. Appl. Phys.* **2001**, *89*, 5815.
[2] W. G. Schmidt, *Appl. Phys. A* **2002**, *75*, 89.
[3] S.-H. Wei, A. Zunger, *Appl. Phys. Lett.* **1998**, *72*, 2011.
[4] Y.-H. Li, A. Walsh, S. Chen, W.-J. Yin, J.-H. Yang, J. Li, J. L. F. Da Silva, X. G. Gong, S.-H. Wei, *Appl. Phys. Lett.* **2009**, *94*, 212109.
[5] A. Schleife, F. Fuchs, C. Rödl, J. Furthmüller, F. Bechstedt, *Appl. Phys. Lett.* **2009**, *94*, 012104.
[6] C. Mitra, B. Lange, C. Freysoldt, J. Neugebauer, *Phys. Rev. B* **2011**, *84*, 193304.
[7] B. Höffling, A. Schleife, C. Rödl, F. Bechstedt, *Phys. Rev. B* **2012**, *85*, 035305.
[8] M. M. May, H. J. Lewerenz, D. Lackner, F. Dimroth, T. Hannappel, *Nat. Commun.* **2015**, *6*, 8286.
[9] M. R. Lorenz, G. D. Pettit, R. C. Taylor, *Phys. Rev.* **1968**, *171*, 876.
[10] R. G. Humphreys, U. Rössler, M. Cardona, *Phys. Rev. B* **1978**, *18*, 5590.
[11] H. C. C. Casey, M. B. Panish, *Heterostructure Lasers, Part A: Fundamental Principles*, Academic Press, New York, NY **1978**.
[12] P. Rochon, E. Fortin, *Phys. Rev. B* **1975**, *12*, 5803.
[13] K. Alberi, B. Fluegel, M. A. Steiner, R. France, W. Olavarria, A. Mascarenhas, *J. Appl. Phys.* **2011**, *110*, 113701.
[14] D. A. Beaton, T. Christian, K. Alberi, A. Mascarenhas, K. Mukherjee, E. A. Fitzgerald, *J. Appl. Phys.* **2013**, *114*, 203504.
[15] A. Abdollahi, M. M. Golzan, *J. Mater. Sci.* **2016**, *51*, 7343.
[16] F. Flores, C. Tejedor, *J. Phys. C: Solid State Phys.* **1979**, *12*, 731.
[17] J. Tersoff, *Phys. Rev. B* **1984**, *30*, 4874.
[18] C. Van de Walle, *Phys. Rev. B* **1989**, *39*, 1871.
[19] C. Van de Walle, J. Neugebauer, *Nature* **2003**, *423*, 626.
[20] M. Landmann, E. Rauls, W. G. Schmidt, M. Röppischer, C. Cobet, N. Esser, T. Schupp, D. J. As, M. Feneberg, R. Goldhahn, *Phys. Rev. B* **2013**, *87*, 195210.
[21] M. Landmann, E. Rauls, W. G. Schmidt, *Phys. Rev. B* **2017**, *95*, 155310.
[22] G. Kresse, J. Furthmüller, *Comput. Mat. Sci.* **1996**, *6*, 15.
[23] J. P. Perdew, A. Ruzsinszky, G. I. Csonka, O. A. Vydrov, G. E. Scuseria, L. A. Constantin, X. Zhou, K. Burke, *Phys. Rev. Lett.* **2008**, *100*, 136406.
[24] J. Heyd, G. E. Scuseria, M. Ernzerhof, *J. Chem. Phys.* **2003**, *118*, 8207.
[25] P. E. Blöchl, *Phys. Rev. B* **1994**, *50*, 17953.
[26] G. Kresse, D. Joubert, *Phys. Rev. B* **1999**, *59*, 1758.
[27] P. V. C. Medeiros, S. Stafström, J. Björk, *Phys. Rev. B* **2014**, *89*, 041407.
[28] O. Madelung, *Semiconductors: Group IV Elements and III–V Compounds (Data in Science and Technology)*, Springer, Berlin **2013**.

© 2020 The Authors. Physica Status Solidi B published by Wiley-VCH GmbH